CKJ REVIEW

Morphometric analysis of chronicity on kidney biopsy: a useful prognostic exercise

Muhammad S. Asghar[1], Aleksandar Denic [1] and Andrew D. Rule[1,2]

[1]Division of Nephrology and Hypertension, Mayo Clinic, Rochester, MN, USA and [2]Division of Epidemiology, Mayo Clinic, Rochester, MN, USA

Correspondence to: Andrew D. Rule; E-mail: rule.andrew@mayo.edu

ABSTRACT

Chronic changes on kidney biopsy specimens include increasing amounts of arteriosclerosis, glomerulosclerosis, interstitial fibrosis and tubular atrophy, enlarged nephron size, and reduced nephron number. These chronic changes are difficult to accurately assess by visual inspection but are reasonably quantified using morphometry. This review describes the various patient populations that have undergone morphometric analysis of kidney biopsies. The common approaches to morphometric analysis are described. The chronic kidney disease outcomes associated with various chronic changes by morphometry are also summarized. Morphometry enriches the characterization of chronicity on a kidney biopsy and this can supplement the pathologist's diagnosis. Artificial intelligence image processing tools are needed to automate the annotations needed for practical morphometric analysis of kidney biopsy specimens in routine clinical care.

Keywords: CKD, glomerulosclerosis, interstitial fibrosis, kidney biopsy, nephrectomy

INTRODUCTION

Morphometry is a technique utilized for the analysis of the spatial distribution and size of tissue structures. In practice, it is accomplished using quantitative image analysis by first annotating with a computer program the different microstructures on whole slide images of stained histological sections of tissue biopsies magnified with light microscopy [1]. The annotations are typically outlines of the individual microstructures seen for a particular class (e.g. glomerular tufts, proximal tubules, or arteries) on whole slide images of tissue biopsies. Annotations can also be applied to the ultrastructures on tissue biopsies magnified with electron microscopy images. Computational pathology uses these computer-assisted electronic annotations to determine counts and areas for each microstructure or ultrastructure. The counts and areas are then used to estimate quantitative measures such as the size or density of different structures on the tissue biopsy. As these annotations are typically two-dimensional, stereological models are often used to estimate the three-dimensional properties of the microstructures from two-dimensional annotations. A common problem is the variable orientation of tubular structures on two-dimensional sections. For example, the minor axis of the tubule profile can be used to approximate the true diameter of a tubular structure (e.g, proximal tubule diameter) [2]. Another approach is to average across multiple structures if the orientations are reasonably 'random' such that the area of these individual structures is reflective of the average orientation (e.g. average cross-sectional tubular area) [3].

Kidney histological sections have gained a particular interest in the application of morphometric analyses due to the characteristic organization of nephrons, the spatial distribution of different microstructures, and the biological importance of the size and density of microstructures [4].
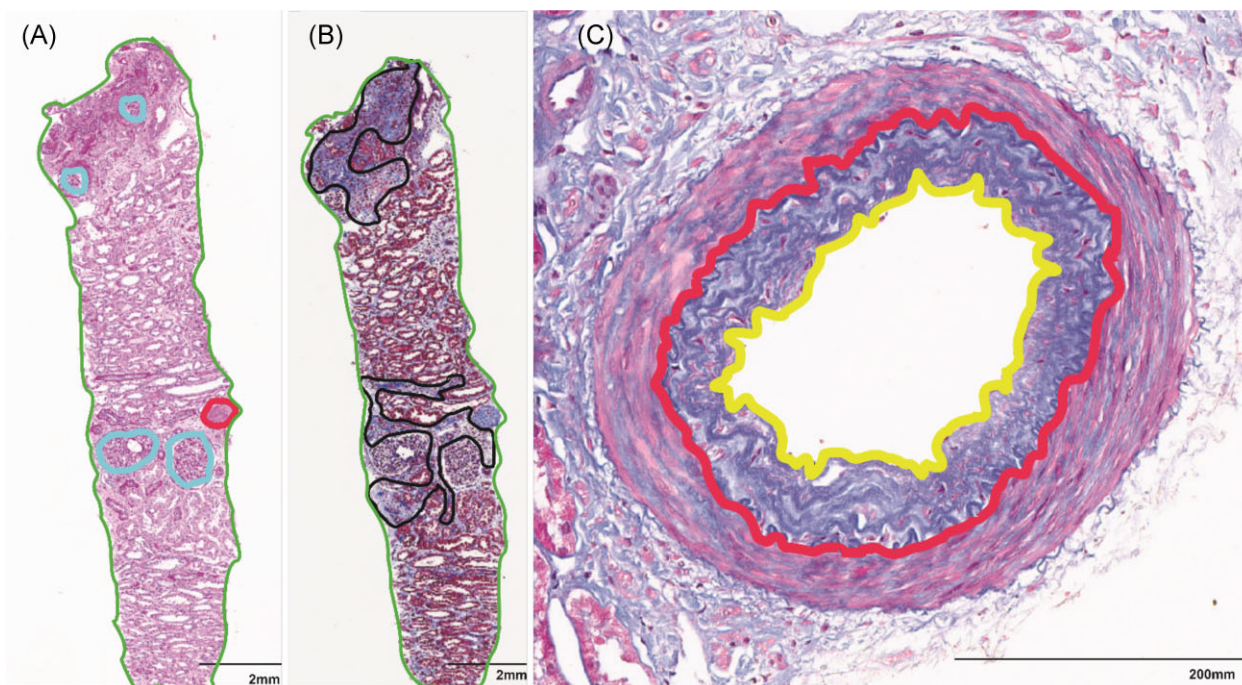
Figure 1: Example of morphometry to assess nephrosclerosis. (A) An example of the annotations needed to estimate % globally sclerotic glomeruli (GSG) with GSG traced in red and non-sclerotic glomeruli (NSG) in cyan. The %GSG is calculated by the number of GSG divided by the total number of glomeruli. The %IFTA is calculated from area of all IFTA foci divided by cortex area. The IFTA foci density is calculated from counts of all IFTA foci divided by cortex area (per cm^2). **(B)** An example of the annotations needed to estimate % interstitial fibrosis and tubular atrophy (IFTA) with IFTA traced in black and cortex traced in green. **(C)** An example of the annotation needed to estimate %luminal stenosis with lumen traced in yellow and intimal thickening traced in red. Arteriosclerosis is assessed by %luminal stenosis from intimal thickening as calculated from the area of intima divided by the areas of intima and lumen.

Morphometry has been widely applied in kidney tissue to quantify chronic changes in the glomerular, tubulointerstitial, and vascular compartments and to monitor progression in patients with repeat biopsies [4]. Figure 1 is an example of the annotations needed to estimate % globally sclerotic glomeruli (GSG), % interstitial fibrosis and tubular atrophy (IFTA), and % artery luminal stenosis from arteriosclerosis (intimal thickening). An important advantage of applying morphometry to detect chronic changes is standardization. In particular, the common scoring of chronic changes on kidney biopsy is often inaccurate and there is limited agreement between different pathologists scoring chronic changes [5–7]. Morphometry can also provide a continuous score that detects subtle variation in mild chronic changes missed by visual inspection. For example, %IFTA of 2% versus 8% is often grouped together as <10% by visual inspection scoring [8]. This is further complicated by the need for thresholds that increase with age for chronic changes that distinguish abnormal from normal [9].

While morphometry is used as a research tool, it has not been routinely used in clinical workflows to evaluate kidney biopsies as it is tedious and time consuming. Morphometry may also oversimplify kidney structures into a set of quantitative measures that do not account for all important pathological findings of the structures. For example, an estimate of percentage globally sclerotic glomeruli (GSG) does not account for whether the GSG have a solidification or ischemic subtype [10]. This is clinically important as solidification is always due to disease whereas ischemic GSG also occur in healthy aging [9]. Morphometry can also be inaccurate due to biopsy quality, over- or under-staining, or inadequate tissue sample to make precise measures. However, these same factors can also affect kidney biopsy assessments by visual inspection. This review focuses on the application of morphometry to clinical biopsies of the kidney and its prognostic significance. The review was based on both our knowledge of this field and a literature search using PubMed, Ovid MEDLINE, and Google Scholar. The following search terms were used: ('Renal Biopsy') AND ('morphometry') AND ('prognosis' OR 'chronicity' OR 'diagnosis' OR 'management' OR 'treatment').

KIDNEY BIOPSY MORPHOMETRY STUDY TYPES

Kidney biopsy morphometry has been applied to study different specific patient populations (Table 1). Morphometry has also been used to study microstructures and pathology that is prognostic for kidney failure or related outcomes (Table 2). Reviewing published studies, Periodic acid-Schiff (PAS) stained biopsy images appear to be the most common used in analyses, followed by Masson's trichrome stained biopsy images. Staining with PAS has been generally preferred by most studies due to stain quality being more uniform across different histopathologic laboratories. While more labor intensive and requiring experienced laboratory technicians, some pathologists prefer Jones' silver stain for %IFTA [11, 12]. Of particular interest is whether morphometric measures are prognostic for outcomes independent of concurrent clinical assessment of kidney function (particularly GFR and proteinuria) and CKD risk factors (particularly hypertension, diabetes, and obesity). Such analyses are helpful for determining whether microstructural pathology is prognostic for outcomes along pathways not well detected by current clinical

Table 1: Studies using morphometry to identify chronic changes on kidney biopsy in order to characterize specific patient populations.

Authors	Study population	Morphometry measures	Sample size	Image software used for morphometry
Marini et al. [56]	FSGS, MCNS, lupus nephritis, Berger's disease, Alport's syndrome, membranous glomerulopathy, ADGN	Bowman's capsule area and glomerular tuft area	59 cases	Leica QWin® (Wetzlar, Germany)
Sharma, et al. [57]	FSGS, mesangioproliferative glomerulonephritis, MCNS, interstitial nephritis	Glomerular basement membrane thickness, endothelial fenestration, slit pore diameter, and foot process width	11 cases	analySIS ProTM software (Soft Imaging System, Muenster, Germany)
Gupta, et al. [58]	Lupus nephritis	Non-inflammatory arteriolar changes: wall thickness, circumference, and wall-to-lumen ratio	40 cases 40 controls	ImageProPlus software (Media Cybernetics Inc., Rockeville, USA)
Das et al. [59]	Idiopathic FSGS	Glomerular area, segmental categorization of glomerular sclerosis, hyalinosis, capsule adhesion, mesangial proliferation, interstitial foam cells, and prominence of visceral epithelial cells	65 cases	Image ProPlus software (Media Cybernetics, Bethesda, MD, USA)
Derewicz et al. [60]	MCNS, FSGS, lupus nephritis, membranous nephropathy, and proliferative extracapillary glomerulonephritis	Glomerular cross-sectional area and mean value diameter	30 cases 30 controls	Leica (Digital Image Hub, version 4.0.6)
Kashif et al. [61]	MCNS, FSGS, HSP, IgA nephropathy, lupus nephritis, Alport syndrome	Bowman's capsule area, glomerular capillary tuft area, and Bowman's space area	28 cases 10 controls	Dewinter Biowizard 4.1 image analysing software
Athanazio et al. [62]	Lupus nephritis	Mesangial hypercellularity, endocapillary proliferation, glomerulosclerosis, tubular atrophy, and interstitial fibrosis	33 cases 20 controls	ImageProPlus, Media Cybernetics
Danilewicz et al. [63]	Cases: Obesity-related FSGS; and Controls: idiopathic FSGS	Total glomerular area, total glomerular cells, mesangium, and interstitial volume	99 cases 15 controls	MultiScan 8.08 software, Computer Scanning Systems, Poland
Smoyer et al. [64]	MCNS, IgM nephropathy, FSGS	Renal scarring as segmental glomerular, global glomerular, and interstitial	15 cases 8 controls	IP Lab Spectrum software (Signal Analytic, Vienna, Va., USA)
Sasaki et al. [65]	Steroid-sensitive MCNS	Nephron number and volumetric nonsclerotic glomerular density	75 cases	Win Roof 2017 image-analysis software (Mitani Corp)
Gupte et al. [66]	Cyanotic nephropathy	Glomerulomegaly, glomerulosclerosis, periglomerular fibrosis, hyperplastic arteriolosclerosis, and interstitial fibrosis	50 cases 25 controls	Imagepro Express software (Media Cybernetics, Silver Spring, MD, USA)
Rayat et al. [67]	MCNS, idiopathic membranous glomerulonephritis, thin basement membrane disease, and Alport's syndrome	Glomerular diameter/area, tuft diameter/area, glomerular volume fraction, capillary space volume fraction, mesangial matrix volume fraction, and capillary space volume fraction	10 cases 10 controls	Quantimet-600 image analysis system (Leica, Cambridge, United Kingdom)

Table 1: (Contiuned)

Authors	Study population	Morphometry measures	Sample size	Image software used for morphometry
Tsuboi et al. [23]	IgA nephropathy	Total glomerular number, global sclerosis, cellular/fibrocellular crescent, glomerular capsular adhesion, mesangial proliferation/matrix, intracapillary proliferation, segmental glomerular sclerosis, interstitial fibrosis, renal cortical (excluding interstitial fibrosis), glomerular density, maximum glomerular area, and mean glomerular area	18 cases	Scion Image (computed imaging analyser)
Koike et al. [21]	Focal segmental glomerulosclerosis, or minimal change disease	Total glomerular number, total cortical area, %IFTA, global glomerular sclerosis, focal segmental sclerosis, glomerular volume, and density	31 cases	
Haruhara et al. [32]	Autopsy kidneys	Nephron number, podocyte density, podocyte number, podocyte volume, and glomerular volume	50 cases	
Okabayashi et al. [39]	Autopsy kidneys	Mean glomerular volume, global glomerulosclerosis, arteriosclerotic lesions, arteriolar hyalinosis, and IFTA	59 cases	
Kanzaki et al. [68]	Autopsy kidneys	Glomerular number (sclerosed and non-sclerosed), cortical and glomerular volume	27 cases	
Haruhara et al. [26]	Hypertensive nephropathy	Glomerulosclerosis (global/segmental), collapsed glomeruli, IFTA, glomerular density, and the presence of arterial and arteriolar lesions	58 cases	Leica IM500, computer image analyzer (Leica Microsystems, Wetzlar, Germany)
Okabayashi et al. [30]	Obesity-related glomerulopathy	Non-sclerotic glomeruli, segmental/global glomerulosclerosis, area of interstitial fibrosis/tubular atrophy, mean glomerular capillary area, mean glomerular volume, and nonsclerotic glomerular density	48 cases	Aperio Image Scope 12.4 (Leica Microsystems, Wetzlar, Germany)
Sasaki et al. [25]	Autopsy kidneys	Glomerular volume, global/nodular glomerulosclerosis, mesangial expansion, arteriolar hyalinosis, doubling of glomerular basement membrane contour, and mesangiolysis	82 cases	Leica IM500, computer image analyzer (Leica Microsystems, Wetzlar, Germany)
Tsuboi et al. [27]	Native kidney biopsies	Mean glomerular volume and glomerular density	206 cases	
Koike et al. [42]	Minimal change disease	Total glomerular number, total cortical area, % global/segmental glomerular sclerosis, % interstitial fibrosis, glomerular volume, and density	50 cases	Leica IM500, computer image analyzer (Leica Microsystems, Wetzlar, Germany)
Kobayashi et al. [69]	Recipients of kidney transplant	Glomerular volume and density	36 cases	Scion Image (computed imaging analyser)
Hamada et al. [70]	Recipients of kidney transplant	Arteriolar expression of endothelial cells of <150 um diameter	50 cases	Olympus BX51 (Olympus, Tokyo, Japan)
Yamakawa et al. [71]	Donors and recipients of kidney transplant	Glomerular area, volume and density, glomerulosclerosis, and %IFTA	23 cases	Scion Image (computed imaging analyser)
Sasaki et al. [14]	Living kidney donors	Non-sclerotic and total glomerular number, mean glomerular tuft area and volume	44 cases	Leica IM500 (Leica Microsystems, Germany)
Sasaki et al. [13]	Living kidney donors and native kidney biopsies	Measured cortical volume, non-sclerotic, and total glomerular density	107 cases	Leica IM500 (Leica Microsystems, Germany)
Sasaki et al. [36]	Living kidney donors	Bowman's capsule volume and glomerular capillary volume, global sclerosis, and interstitial fibrosis	37 cases	Leica IM500 (Leica Microsystems, Wetzlar, Germany)

Table 1: (Continued)

Authors	Study population	Morphometry measures	Sample size	Image software used for morphometry
Marumoto et al. [72]	IgA nephropathy	Non-globally sclerotic and globally/segmental sclerotic glomeruli, glomeruli with cellular/fibrocellular crescents, arteriosclerotic lesions and arteriolar hyalinosis, and %IFTA	245 cases	Win Roof 2017 (Mitani Corporation, Tokyo, Japan)
Oba et al. [73]	Living kidney donors	Total number of glomeruli, mean glomerular tuft area, and volume, cortical area, % glomerulosclerosis, and % IFTA	43 cases	Leica IM500 (Leica Microsystems, Wetzlar, Germany)
Okabayashi et al. [74]	Grade 1 obesity with proteinuria vs living kidney donors	Non-sclerosed and total glomerular number, glomerular volume, % of glomeruli affected by global/segmental sclerosis, %IFTA, arterial and arteriolar lesions	51 cases	Leica IM500 (Leica Microsystems, Wetzlar, Germany)
Tsuboi et al. [28]	Autopsy kidneys (with obesity-related glomerulopathy), IgA nephropathy, and living kidney donors	Glomerular density and glomerular volume, % of glomeruli affected by global/segmental sclerosis, and %IFTA	138 cases	Leica IM500 (Leica Microsystems, Wetzlar, Germany)
Okamoto et al. [29]	Native kidney biopsies (with proteinuria)	Globally sclerosed glomeruli, segmentally sclerosed glomeruli, interstitial fibrosis, arteriolar hyalinosis, arterial fibrous intimal thickness, and glomerular density	34 cases	Leica IM500 (Leica Microsystems, Germany)
Haruhara et al. [38]	Living kidney donors	Kidney cortical volume, Non-sclerotic, and total nephron number, glomerular volume, diameters of podocyte nuclei, podocyte density/number per glomerular tuft, podocytic nuclear/cytoplasmic volume and ratio	50 cases	Fiji open-source software (ImageJ)
Lopes et al. [35]	Living kidney donors	Cortical interstitial volume fraction, cortical glomerular volume fraction, mean glomerular volume, glomerulosclerosis, mean and maximal intimal arterial volume fraction, and of the largest artery	77 cases	Aperio Image Scope software (Version 12.2.2.5015; Leica Microsystems, Germany)
Denic et al. [53]	Living kidney donors	Nonsclerotic glomerular volume, GSG volume and %, tubular cross-sectional area, cortical area, % artery luminal stenosis, and % interstitial fibrosis	1638 cases	Aperio Image Scope software (Version 12.2.2.5015; Leica Microsystems, Germany)
Kremers et al. [41]	Living kidney donors	Number of glomeruli/globally sclerotic glomeruli/non-sclerotic glomeruli/ischemic non-sclerotic glomeruli, and interstitial fibrosis	2052 cases	Aperio Image Scope software (Version 12.2.2.5015; Leica Microsystems, Germany)
Denic et al. [15]	Living kidney donors	Nonsclerotic glomerular volume, tubular area, glomerulosclerosis, arteriosclerosis, Interstitial fibrosis, and nephron number	1388 cases	Aperio Image Scope software (Version 12.2.2.5015; Leica Microsystems, Germany)
Denic et al. [24]	Living kidney donors and radical nephrectomy biopsies	NSG number and tuft volume, GSG number and volume, ischemic appearing NSG, % interstitial fibrosis, and % artery luminal stenosis	3233 cases	Aperio Image Scope software (Version 12.2.2.5015; Leica Microsystems, Germany)
Denic et al. [31]	Radical nephrectomy biopsies	Cortex area, NSG number and tuft volume, GSG number and volume, and ischemic appearing NSG number and volume	812 cases	Aperio Image Scope software (Version 12.2.2.5015; Leica Microsystems, Germany)
Wavamunnoo et al. [75]	Transplant protocol biopsies (taken at implantation, 1, 3, 6, and 12 months and then annually until 5 years)	Acute glomerulitis, interstitial fibrosis, tubular atrophy, acute tubular necrosis, chronic vascular changes, arteriolar hyalinosis mesangial matrix, and podocyte foot process effacement (on EM analysis)	228 biopsies from 15 patients	Soft Imaging Systems, analySIS, GmBh, Germany)
Howie et al. [76]	IgA nephropathy, Henoch Schoenlein nephritis, vasculitic glomerulonephritis, minimal change nephropathy, segmental sclerosing diseases, thin glomerular basement membrane disease, membranous nephropathy	Global sclerosis, areas of interstitial fibrosis and atrophic tubules, arteries and arterioles completely occluded were judged to have chronic damage.	247 cases	Aequitas IA image analysis software (Dynamic Data Links, Cambridge, UK)

ADGN: acute diffuse glomerulonephritis; CCHD: cyanotic congenital heart disease; FSGS: focal segmental glomerulosclerosis; IFTA: interstitial fibrosis and tubular atrophy; MCNS: minimal change nephrotic syndrome.

Table 2: Studies using morphometry to quantify chronic changes on kidney biopsies in order to predict CKD outcomes.

Authors	Study population	Morphometric measurements	Associates with CKD outcomes	Image software	Sample size
Denic et al. [5]	Native kidney biopsies	Cortex area, glomerular volume, cortex volume per glomerulus, non-IFTA cortex volume per glomerulus, %ischemic-appearing glomeruli, %segmentally sclerosed glomeruli, %GSG, %IFTA, IFTA foci density, %luminal stenosis, arteriolar hyalinosis and %interstitial inflammation	Glomerular volume, %GSG, %IFTA, IFTA foci density, and arteriolar hyalinosis	Aperio ImageScope software (version 12.4.3; Leica Microsystems, Germany)	353
Hunter et al. [77]	Lupus nephritis	nuclear index, tubular space, collagenous matrix, and fibrillary collagen	High collagen matrix and tubular space	Openlab 3.0.0 software; Improvision, Lexington, MA, USA; and Image J 1.30; National Institutes of Health, Bethesda, MD, USA	48
Voila et al. [78]	IgA nephropathy and MCNS	Glomerular capillary loops, endothelial cells, and interstitial macrophages	Interstitial macrophages	MetaMorph Software System (Universal Imaging Corp Molecular Device Corp, CA, USA)	44
Lemley et al. [79]	FSGS, MCNS, membranous nephropathy	Mean glomerular tuft area, cortical density of patent glomeruli, interstitium, atrophic tubule, intact tubule, blood vessel, sclerotic glomerulus, and patent glomerulus	Fraction atrophic tubule	SlidePath server (Leica MicroSystems, Dublin)	56
Paraskevakou et al. [80]	Idiopathic membranous glomerulonephritis	Surface area, perimeter, major axis length, shape factor of renal glomeruli, and percentage of the interstitial fibrosis	Percentage of interstitial fibrosis	SigmaScan v.2.0 software (Jandel Scientific Corp); and ColorEstimator v.2.0, (Microsoft Visual Basic 5.0 environment)	45
Horvatic et al. [81]	Idiopathic membranous glomerulonephritis	Glomerular area, tuft area, mesangial area, urinary space area, capillary space area, glomerular diameter, tuft diameter, tuft volume fraction, urinary space volume fraction, mesangial volume fraction, capillary space volume fraction, glomerular basement membrane thickness, glomerulopathy index, and %IFTA	%IFTA	ImageJ image analysis software	60
Fufaa et al. [82]	Type 2 diabetes	Global glomerular sclerosis, mean glomerular volume, glomerular basement membrane width, cortical interstitial fractional volume, mesangial fractional volume per glomerulus, glomerular filtration surface density, total filtration surface per glomerulus, nonpodocyte no. per glomerulus, podocyte no. per glomerulus, foot process width, podocyte detachment, and endothelial fenestration	Global glomerular sclerosis, mean glomerular volume, glomerular basement membrane width, glomerular filtration surface density, mesangial fractional volume per glomerulus, nonpodocyte no. per glomerulus, foot process width, and endothelial fenestration		111
Tsuboi et al. [22]	IgA nephro-pathy	Total glomerular number, total cortical area, global/segmental glomerular sclerosis, mesangial proliferation, %IFTA, cellular/fibrocellular crescent, mean glomerular volume, and glomerular density	Cellular/fibrocellular crescent and glomerular density	Scion Image (computed imaging analyser)	98

Table 2: (Continued)

Authors	Study population	Morphometric measurements	Associates with CKD outcomes	Image software	Sample size
Amano et al. [44]	Benign nephrosclerosis	Glomerular number, global glomerulosclerosis, and %IFTA	Glomerulosclerosis and %IFTA		98
Tsuboi et al. [43]	Idiopathic membranous nephropathy	Total cortical area. total glomerular number, global/segmental glomerular sclerosis, %IFTA, glomerular density	Glomerular density	Scion Image (computed imaging analyser)	65
Haruhara et al. [37]	Biopsy-proven nephrosclerosis	Mean volumes for glomerular tufts and Bowman's capsules, number of Bowman's capsules lacking glomerular tufts, glomerular density, global/segmental glomerulosclerosis, periglomerular fibrosis, %IFTA, and arteriolar hyalinosis index	G/B ratio (glomerular volume to Bowman's space volume ratio)	Leica IM500 (Leica Microsystems, Germany)	67
Issa et al. [18]	Living kidney donors	Cortex volume per glomerulus, glomerular volume, tubular cross-sectional area, globally sclerotic glomeruli, %IFTA, IFTA foci density, % artery luminal stenosis, and nephron number	Glomerular volume and number of IFTA foci	Aperio Image Scope software (Version 12.2.2.5015; Leica Microsystems, Germany)	2673
Merzkani et al. [34]	Living kidney donors	Nephron number, glomerular volume, cortex volume per glomerulus, mean tubular cross-sectional area, %GSG, IFTA foci density, %IFTA, artery luminal stenosis, arteriolar hyalinosis	Glomerular volume, cortex volume per glomerulus and nephron number	Aperio Image Scope software (Version 12.2.2.5015; Leica Microsystems, Germany)	807
Hommos et al. [45]	Focal segmental glomerulosclerosis, membranous nephropathy, and minimal change disease	Number of glomeruli, number and % of GSG, cortical IFTA, arteriolar hyalinosis, and arteriosclerosis	GSG abnormal for age		425
Denic et al. [54]	Recipients of kidney transplant	%fibrosis area, mesangial expansion, artery luminal stenosis, and arteriolar hyalinosis	Mesangial expansion and % arteriosclerosis	Aperio Image Scope software (Version 12.2.2.5015; Leica Microsystems, Germany)	201
Niznik et al. [40]	Living kidney donors	Cortical area, nephron number, number of glomeruli, glomerular volume, and cortex volume per glomerulus, %IFTA and foci density, and %luminal stenosis	Nephron number, glomerular volume, and cortex volume per glomerulus	Aperio Image Scope software (Version 12.2.2.5015; Leica Microsystems, Germany)	2915
Issa et al. [33]	Kidney donor biopsies predicting graft failures in recipients	Cortical volume per glomerulus, nonsclerotic glomeruli volume, %globally sclerotic glomeruli, %IFTA, IFTA foci density, %artery luminal stenosis, tubular cross-sectional area, and arteriolar hyalinosis	Glomerular volume, tubular cross-sectional area, and IFTA	Aperio Image Scope software (Version 12.2.2.5015; Leica Microsystems, Germany)	2293
Denic et al. [46]	Recipients of kidney transplant	Glomerular volume, %GSG and %ischemic glomeruli	%GSG and ischemic glomeruli	Aperio ImageScope software (version 12.4.3; Leica Microsystems, Germany)	835
Denic et al. [3]	Radical nephrectomy biopsies	Cortex area, NSG number, and volume, cortex volume per glomerulus, %GSG, %IFTA, IFTA foci density, tubular cross-sectional area, and % artery luminal stenosis	Glomerular volume, %GSG, tubular cross-sectional area, %IFTA, and IFTA foci density	Aperio Image Scope software (Version 12.2.2.5015; Leica Microsystems, Germany)	936

EM: electron microscopy; GSG: globally sclerosed glomeruli; IFTA: interstitial fibrosis and tubular atrophy; NSG: non-sclerosed glomeruli.

assessments of kidney health. These analyses clarify the added value of kidney biopsy to the prognostic assessment of various patient populations.

The 'unselect' general population would be of particular interest with respect to prognosis with various kidney microstructural morphometry measures on kidney biopsy. However, due to the invasive nature of kidney biopsies, such a study is not feasible. All human kidney biopsy studies require some clinical justification for obtaining a kidney biopsy. This inherently leads to selection bias as abnormal kidney function (particularly proteinuria) influences the selection of patients that undergo a kidney biopsy. Living kidney donation and radical nephrectomy for kidney tumor are the unique setting in medicine where a kidney biopsy can be obtained intraoperatively (low risk of bleeding complication) and obtained in patients not selected on abnormal kidney function. As both these populations undergo a nephrectomy, repeat kidney function assessment over time after the nephrectomy often occurs as part of follow-up care.

Living kidney donors are subjected to a thorough predonation examination of their overall and kidney health status before the actual donation. Given the requirement of normal kidney function and the presence of relatively low chronic kidney disease (CKD) risk factor burden prior to kidney donation, donors provide a particularly useful setting for understanding the normal age-related changes that occur in healthy kidneys. Kidney tumor patients that undergo a radical nephrectomy have more CKD risk factors and abnormal kidney function as a population than living kidney donors. Similar to donors, they are also not selected on abnormal kidney function to justify a kidney biopsy. Large wedge sections of the non-tumor parenchyma from radical nephrectomy specimens allow unique study of kidney tissue specimens with 20-fold more cortex than the typical needle core biopsies. Large wedge sections also allow for morphometric study of microstructural patterns that may vary by depth, a factor that is difficult to discern from needle core biopsies.

NEPHRON SIZE AND NUMBER

Several studies have utilized morphometry evaluation of both kidney biopsy images and computed tomography or magnetic resonance kidney images to calculate the nephron number from the density of glomeruli in the cortex multiplied with the total volume of cortex per kidney [13–17]. Low nephron number predicts adverse kidney function outcomes in both living kidney donors and tumor patients [16, 18]. Nephron number and nephron size have a reciprocal relationship due to compensatory enlargement of nephrons with low nephron endowment or nephron loss due to aging and disease. Because radiographic kidney imaging that can accurately delineate cortical volume is often not available, nephron number is not available in most patients that undergo kidney biopsy. While renal pathology reports will comment on glomerulomegaly when severe, more subtle manifestations of nephron enlargement may go unnoticed by visual inspection alone. Morphometry can estimate nephron size in a more standardized and quantitative manner. In particular, nephron size can be assessed by measures of non-sclerosed glomerular volume or by cortex volume per non-sclerosed glomerulus (reciprocal of glomerular density). Morphometric assessment of glomerular volume and glomerular density can be performed from the areas of glomerular profiles and cortex using the Weibel–Gomez stereological model, though this approach effectively assumes the size of different glomeruli are relatively similar [19]. An explanation of the un-
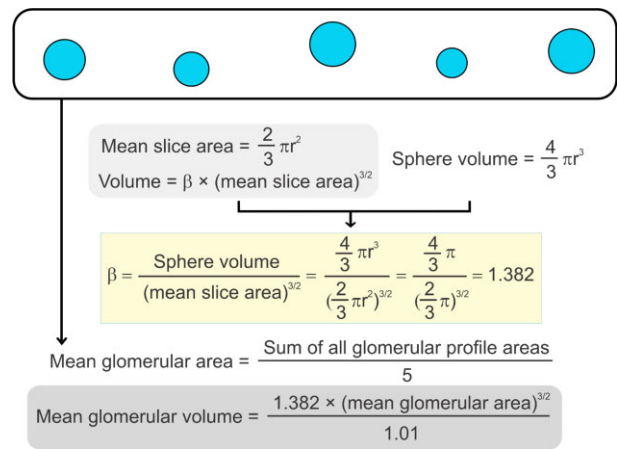

Figure 2: Calculation of glomerular volume. A hypothetical example of a biopsy with five glomerular profiles is shown. Light gray shaded box shows Weibel and Gomez stereology model for random slices of spheres [17]. The yellow box shows derivation of 1.382, the coefficient for spheres. If we model glomeruli as spheres, the mean glomerular profile area is used as the mean slice area. The darker gray shaded box shows how glomerular volume is calculated. This formula also uses a coefficient of 1.01 to account for an estimated coefficient of variation of 10% for glomerular diameters across multiple glomeruli in a patient [18].

derlying math used to calculate the mean volume of glomeruli on a kidney biopsy section is shown in Fig. 2 [17].

There are several clinical characteristics associated with nephron number and nephron size. Low birth weight is associated with low nephron endowment and enlarged nephrons (larger glomerular volume and lower glomerular density) [20–23]. In a large study of living kidney donors and kidney tumor patients, clinical characteristics that independently associated with larger glomerular volume were family history of end-stage kidney disease (ESKD), male, tall stature, obesity, diabetes, and proteinuria [24]. Larger glomeruli were also associated with more globally sclerotic glomeruli and with modest increases in interstitial fibrosis consistent with compensatory enlargement of remaining nephrons with nephrosclerosis [24]. An autopsy study also found diabetes and hypertension independently associate with larger glomerular volume [25]. In biopsy-proven hypertensive nephropathy, low glomerular density correlated with overt proteinuria [26]. The association of enlarged nephrons (larger glomerular volume or lower glomerular density) with higher BMI or obesity has been well described in many studies and patient populations [27–29]. An increase in single nephron GFR is also associated with enlarged glomeruli [30].

Glomerular volume and its clinical associations can also vary by cortical depths. A study of large wedge sections from kidney tumor patients, spanning from the capsule to the corticomedullary junction, found the glomerular volume was largest in the mid cortical region and smallest in the superficial region [31]. Taller stature, obesity, hypertension, diabetes, proteinuria, and current smoking are associated with larger glomerular volume at all cortical depths, but obesity is more strongly associated with glomerular volume in the superficial cortex [31]. Glomerular volume by depth was somewhat different in an autopsy kidney study, where the largest glomerular volume was in deep cortex [32]. However, among patients with preserved kidney function and nephron number, glomerular volume was larger in both the middle and deep cortex compared to the superficial cortex [32].

Table 3: Risk of CKD outcomes with morphometric of measures of chronic changes across different populations.

Morphometric measures	Donor biopsy predicting outcome in donor	Recipient biopsy predicting outcome in recipient	Donor biopsy predicting outcome in recipient	Kidney tumor patients	Native kidney disease disease patients
Nephron size and number					
Glomerular volume	↑[18][a] [34],[a]	↓[46][b]	↑[35][a] [33],[a]	↑[3][a]	↑[5][a]
Cortex volume per glomerulus	↔[18][a], ↑[34][a]		↔[33][a]		↑[22][a]
Tubular cross-sectional area	↔[18][a] [34],[a]		↑[33][a]	↔[3][a]	↑[5][a]
Nephron number	↔[18][a], ↓[34][a],↓[14][a]		↔[33][a]	↔[3][a],↓[14][a]	
Glomerulosclerosis					
%GSG	↔[18][a] [34],[a]	↑[46][b]	↔[33][a]	↑[3][a]	↑[44][a] [5],[a], ↔[22][a]
Mesangial expansion		↑[54][b]			↔[81][b] [22],[a]
Ischemic glomeruli		↑[46][b]			
IFTA and interstitial inflammation					
%IFTA	↔[18][a] [34],[a]	↔[54][b]	↑[33][a]	↑[3][a] [50],[a]	↑[81][a] [5],[a], ↔[44][a]
IFTA foci density	↑[18][a], ↔[34][a]		↔[33][a]	↑[50][a]	↑[5][a]
Inflammation				↔[50][a]	↑[5][a]
Arteriosclerosis					
%Artery luminal stenosis	↔[34][a]	↑[54][b]	↔[35][a] [33],[a]	↔[3][a]	↔[5][a]
Arteriolar hyalinosis			[33],[a]		↑[5][a]

↑: Increased risk with higher values of morphometric measure.
↓: Decreased risk with higher values of morphometric measure.
↔ No risk.
[a]Adjusted analysis.
[b]Unadjusted analysis.
Studies reported outcomes as <60 mL/min/1.73 m^2 eGFR [18], some as <45 mL/min/1.73 m^2 eGFR [34], >40% decline in eGFR from baseline [14] [3] [50], >50% decline in eGFR from baseline [5] [22] [81], a 30% decline in eGFR from baseline or end-stage renal disease [44], or graft loss/failure [33] [35] [54] [46].

There is evidence that enlarged nephrons and low nephron number are associated with a worse kidney prognosis in a variety of patient populations. Larger glomerular volume and low nephron number predicted a low GFR early and long-term after kidney donation and graft failure in the recipient [16, 18, 33, 34]. Larger glomerular volume predict outcomes as progressive CKD in several studies with different population [3, 5, 35]. Table 3 summarizes morphometric measures of chronic changes and their prediction of adverse kidney outcomes in living kidney donors, kidney transplant recipients, kidney tumor patients, and native kidney disease patients.

Glomerular volume can be assessed at the tuft or capsule level. The Bowman's (urinary) space between the capsule and tuft can also be studied morphometrically. One study in living kidney donors studied the measurements of all cross-sectional areas and volumes of glomeruli at the capsule and tuft level and defined a ratio between the two (i.e. glomerular tuft volume divided by Bowman's volume or G/B) [36]. While the G/B ratio did not associate with the same risk factors associated with large glomerular volume (e.g. obesity) [36], patients with nephrosclerosis and a low G/B ratio were at increased risk for progressive CKD [37]. A low G/B ratio (or relatively increased Bowman's space) may reflect glomerular hyperfiltration beyond that detected by enlarged glomerular volume alone.

PODOCYTES MORPHOMETRY

Podocyte morphometry usually involves the counts of podocyte per glomerular tuft, podocyte density, and podocyte volume. With aging, most losses of podocytes are due to loss of glomeruli rather than a decrease in podocyte counts among remaining glomeruli [38]. Hypertension associates with lower podocyte density and larger podocyte volume. In living kidney donors, hypertension and aging were associated with lower podocyte count; however, hypertension alone associated with lower podocyte density and larger podocyte volume independent of age [38]. Among normal kidneys at autopsy, those with more nephrons had more podocytes per glomerulus as well as higher podocyte density. While the counts of podocytes did not differ by cortical depth, there was higher podocyte density in superficial glomeruli due to smaller glomeruli and smaller podocytes [32]. Older age was associated with lower podocyte counts, particularly in superficial glomeruli [32], a finding that parallels a higher frequency of glomerulosclerosis among superficial glomeruli but not deep glomeruli with older age [31]. Further studies are needed to understand the prognostic implications of podocyte morphometry.

GLOMERULOSCLEROSIS

The %GSG is perhaps the one morphometric measure that is routinely reported in clinical practice. Glomerular counts can be reported per section or as total count across serial sections, but undercounting of glomeruli by visual inspection alone is a common problem. A morphometric approach ensures standardized counting of glomeruli and inclusion of partial counts for glomeruli bisected by the biopsy needle [16]. Global glomerulosclerosis is evident in both aging and in kidney disease. Among kidney donors, age associated much more strongly with %GSG than did hypertension [39]. It is perhaps not well appreciated that smaller amounts of cortex tissue on a needle core biopsy is itself associated with more glomerulosclerosis on biopsy [40]. This occurs because loss of nephrons itself leads to smaller cortical tissue biopsy samples, though clinical skill and chance are often thought to be the only reasons for inadequate cortex on a needle core biopsy. The upper reference limit (defined as 95th percentile) for the number of globally sclerosed glomeruli (GSG) increases with older age as determined from normotensive living kidney donor biopsies [41]. These thresholds can help distinguish patients who have glomerulosclerosis

due to CKD rather than aging alone. Glomerulosclerosis occurs more in the superficial cortex with age and is accompanied by non-sclerosed glomeruli with an ischemic appearance (capillary wrinking and capsule thickening [31]). Whereas low eGFR, hypertension, and interstitial fibrosis associate with glomerulosclerosis at all cortical depths, and diabetes more strongly associated with glomerulosclerosis in the deeper cortex [31]. Another study on autopsy kidneys found diabetics without hypertension had more glomerulosclerosis in the deep cortex [25].

Numerous studies have linked higher %GSG to a higher risk of adverse kidney outcomes in a variety of patient populations [21, 22, 42, 43]. In patients whose kidney biopsy diagnosis was 'benign nephrosclerosis', %GSG and proteinuria were the most significant predictors of a 30% decline in eGFR from baseline [44]. Among nephrotic syndrome patients, an increased risk of progressive CKD was only evident when the %GSG exceeded age-based thresholds for GSG [41, 45]. Among kidney allografts at a 5-year surveillance biopsy, higher %GSG as well as higher % ischemic-appearing glomeruli were predictive of subsequent allograft loss [46].

INTERSTITIAL FIBROSIS AND TUBULAR ATROPHY

The severity of IFTA is an important prognostic indicator of chronic changes on kidney biopsy that is often inaccurately and imprecisely scored by visual inspection [5]. IFTA occurs on a continuum with mild forms having basement membrane thickening without significant atrophy and minimal surrounding interstitial fibrosis to more mature and severe tubular atrophy with basement membrane disruption and substantial surrounding interstitial fibrosis. Annotation of IFTA is tedious and one approach is to identify and annotate clusters of IFTA foci where atrophic tubules are bunched together and surrounded and connected by interstitial fibrosis. Among the standard stains obtained on clinical biopsies, trichome stained sections are often used to morphometrically assess severity of IFTA. One study found collagen III staining optimal for morphometry with better interobserver reproducibility compared to morphometry by visual inspection [7]. The %IFTA (percentage of cortex area that is IFTA) is often viewed as the best biopsy assessment of CKD; it is notable that it often has rather modest correlation with eGFR [47, 48]. When needle core kidney biopsies are mostly or only medulla, it is worth noting morphometric assessment of %IFTA in cortex and in medulla are correlated, particularly by PAS staining (r = 0.85) [49].

While morphometric assessment of IFTA has largely focused on %IFTA (area of IFTA divided by area of cortex or %IFTA), the IFTA foci count density (number of IFTA foci divided by area of cortex) appears to be just as important for assessing chronic changes in the kidney and their prognosis. One study morphometrically assessed different patterns of IFTA and inflammation on wedge sections of kidney tumor patients including %IFTA, IFTA foci density, %striped IFTA, %subcapsular IFTA, %inflammation, and %subcapsular inflammation [50]. After adjusting for %IFTA, inflammation outside of IFTA predicted a higher risk of CKD progression and non-cancer mortality, while subcapsular inflammation predicted a higher risk of non-cancer mortality [50]. However, neither inflammation outside of IFTA or subcapsular inflammation predicted outcomes after further adjusting for kidney function and CKD risk factors [50]. In renal allografts, inflammation within IFTA is currently regarded as a component of chronic active T cell-mediated rejection [51]. In kidney tumor patients, inflammation within IFTA did not predict outcomes independent of %IFTA [50]. Striped pattern of IFTA may reflect chronic ischemia from calcineurin inhibitor toxicity [52]. In kidney tumor patients, striped pattern of IFTA did not predict outcomes independent of %IFTA [50].

After adjusting for %IFTA and clinical characteristics, only increased IFTA foci density predicted progressive CKD [50], in other words, at the same severity of %IFTA, patients who had more numerous small scattered IFTA foci had a greater risk of progressive CKD than those with fewer and larger IFTA foci. The IFTA foci density showed a pattern of stronger correlation with older age and lower cortical thickness on biopsy and lower cortical volume on CT or MRI imaging. Loss of nephrons is a dynamic process and foci of IFTA progressively atrophy leading to contraction of the kidney cortex. Because progressive atrophy of IFTA foci both decreases %IFTA and increases IFTA foci density, both %IFTA and IFTA foci density are complimentary rather than redundant in assessing IFTA severity. This was further confirmed in a morphometric study of chronic changes on native kidney biopsies [5]. Table 4 summarizes studies of IFTA via manual morphometry.

ARTERIOSCLEROSIS

Arteriosclerosis (due to fibrointimal thickening) and arteriolar hyalinosis leads to nephron ischemia and nephrosclerosis. Morphometric assessment of arteriosclerosis can be determined by severity of luminal stenosis by intimal thickening. One approach is to take the cross-sectional area of intima divided by the combined area of intima and lumen to assess the % luminal stenosis from intimal thickening [53]. When multiple arteries are present the severity of arteriosclerosis can be averaged across arteries or the artery with the most severe arteriosclerosis used for analyses. More work is needed to determine the optimal approach to quantifying arteriosclerosis that is the most prognostic. Other approaches to arteriosclerosis involve intimal thickening being calculated by comparing the thickness of the intima to that of the media in the same segment of the vessel[26]. Importantly, not all needle core kidney biopsies will have a medium to large artery from which luminal stenosis from intimal thickening can be assessed via morphometry. Orientation of artery profiles and partial arteries (bisected by the biopsy needle) can also contribute to bias in the assessment of arteriosclerosis. One approach to deal with tangential sectioning of blood vessels is not to account for the orientation of the vessel in the calculation but using the most orthogonal arteries to the plane of the biopsy available. This has been used successfully to predict outcomes [53].

Morphometric assessment of arteriolar hyalinosis is even less developed. The Banff criteria classify arteriolar hyalinosis based on descriptive categories of no hyalinosis, mild to moderate hyaline thickening in at least 1 arteriole, moderate to severe PAS-positive hyaline thickening in more than 1 arteriole, or severe PAS-positive hyaline thickening in many arterioles [54]. This approach effectively combines number of involved arterioles with the severity of arteriolar hyalinosis among involved arterioles. The non-specific nature of arteriolar hyalinosis in kidney allografts and the possibility of chronic calcineurin inhibitor toxicity complicates the prognostic interpretation of arteriolar hyalinosis [55]. Other approaches for arteriolar hyalinosis consider only the proportion of arterioles exhibiting any hyalinosis categorized into <5%, 5%–25%, and >25% [26] . Arteriolar

Table 4: Summary of studies that morphometrically quantified %IFTA in human kidney biopsies.

Authors	Clinical associations with higher morphometric %IFTA	Image analyser	No. of biopsies	Stain used to detect IFTA
Farris et al. [7]		ImageScope Positive Pixel Count algorithm; and NIH ImageJ	15	Collagen III IHC, Sirius Red, trichrome and periodic acid–Schiff
Archila et al. [50]	Age, male, hypertension, diabetes, BMI, smoking, glomerular volume, %GSG, % luminal stenosis, 24-hr proteinuria, baseline eGFR, and progressive CKD	Aperio Image Scope software (Version 12.2.5015; Leica Microsystems, Germany)	936	Periodic acid–Schiff (PAS)
Keijback et al. [48]		QWin, Leica's Windows-based image analysis tool kit; (Leica, Cambridge, UK)	286	Sirius Red
Farris et al. [49]	Serum creatinine and eGFR	ImageScope Positive Pixel Count (PPC) algorithm; and Aperio microvessel density (MVD) algorithm	67	Collagen III IHC, trichrome, periodic acid–Schiff, CD-34 IHC
Dao et al. [83]	Serum creatinine and graft function	Calopix, (Tribvn Healthcare, Châtillon France)	66	Sirius Red
Wang et al. [84]		Colocalization algorithm (version 9; Aperio Technologies, Inc.); and Microvessel algorithm (Aperio Technologies, Inc.)	123	Masson's trichrome and CD-34 IHC
Zhang et al. [85]	eGFR	Aperio Image Scope software (Leica Biosystems, Germany)	97	Masson's trichrome and CD-34 IHC
Hamada et al. [86]	Posttransplant anemia	National Institutes of Health software ImageJ	62	Picrosirius red and Triple IHC [blue (PDGFR-β); red (CD-34) and brown (α-SMA)]
Tewari et al. [87]	Serum creatinine	Biowizard 4.2 software	40	Masson's trichrome
Asghar et al. [88]	Age, male, diabetes, hypertension, BMI, 24hr proteinuria, glomerular volume, non-IFTA cortex per glomerulus, % arteriosclerosis, and progressive CKD	Aperio ImageScope software (version 12.4.3; Leica Microsystems, Germany)	3020 living kidney donors, 1363 kidney tumor patients, and 314 native kidney biopsies ($n = 4697$ combined)	Periodic acid–Schiff (PAS) and Masson's trichrome

BMI: body mass index; CKD: chronic kidney disease; GFR: glomerular filtration rate; GSG: globally sclerosed glomeruli; IHC: Immunohistochemistry; PDGFR-β: platelet-derived growth factor receptor beta; α-SMA: smooth muscle alpha-actin.

hyalinosis can be further subclassified into concentric lesions or focal (partial) lesions [5].

In living kidney donors, higher levels of arteriosclerosis by morphometric measures of luminal stenosis by intimal thickening in implantation biopsies associated with hypertension at a short-term follow-up visit [18]. However, long-term risk of CKD and incidence of hypertension was neither predicted by morphometric luminal stenosis nor arteriolar hyalinosis in another study [34]. Among kidney tumor patients, after accounting for clinical characteristics (particularly age), morphometric artery luminal stenosis did not predict progressive CKD [3]. However, kidney allograft loss in kidney recipients was predicted by increased morphometric luminal stenosis of arteries [54]. Morphometirc measures of arteriolar hyalinosis is a better predictors of progressive CKD in native kidney disease patients than is artery luminal stenosis from intimal thickening [5]. Kidney cortex thinning from arteriosclerosis can also affect the quality of a kidney biopsy. In particular, presence and severity of arteriosclerosis by morphometric luminal stenosis by intimal thickening is increased when there is less cortex present on a needle core biopsy [40].

CONCLUSION

Morphometry has proved to be a useful tool in quantifying chronic changes (essentially CKD) on kidney biopsy specimens that are prognostic for adverse kidney events such as kidney failure or a progressive decline in eGFR. Advantages of morphometry are better accuracy and reproducibility than visual assessment, and a saved and auditable record of annotations used to quantify severity of structural pathology. The optimal combination of morphometry measures to assess CKD prognosis appears to be one that includes %glomerulosclerosis (GSG, ischemic glomeruli, and segmental sclerosis), %IFTA, IFTA foci density, and presence of any arteriolar hyalinosis. This combination of morphometry measures is superior in predicting progressive CKD and ESKD to commonly used chronicity scores based on visual inspection [5]. A major limitation is that morphometry is tedious and time-consuming.

Implementation in the clinical practice will likely require automation. In particular, artificial intelligence (AI) models are needed to automate the annotation of microstructures followed by computer programs that perform morphometric and stereological calculations. Current limitations for such approaches include small datasets that come from single institutions, which can limit generalizability. Collaboration between institutions for sharing of data can help improve the algorithms leading to better performing models. In addition, quality control of the AI generated annotations by pathologists is needed given the wide spectrum of pathologies and artifacts that occur on whole slide images of kidney biopsy sections. Future studies are needed to determine if the added clinical and prognostic information from morphometric analysis of kidney biopsy images is of sufficient value to justify the computational costs and quality control efforts of applying AI models within a clinical practice workflow.

FUNDING

DATA AVAILABILITY STATEMENT

No new data were generated or analysed in support of this research.

CONFLICT OF INTEREST STATEMENT

None declared.

REFERENCES

1. Amann K. New parameters in kidney biopsy diagnostic-morphometry. *Kidney Blood Press Res* 2000;**23**:181–2.
2. Denic A, Gaddam M, Moustafa A *et al.* Tubular and glomerular size by cortex depth as predictors of progressive chronic kidney disease after radical nephrectomy for tumor. *JASN* 2023;**34**:1535–45. https://doi.org/10.1681/ASN.0000000000000180
3. Denic A, Elsherbiny H, Mullan AF *et al.* Larger nephron size and nephrosclerosis predict progressive CKD and mortality after radical nephrectomy for tumor and independent of kidney function. *JASN* 2020;**31**:2642–52. https://doi.org/10.1681/ASN.2020040449
4. Kashgarian M. The contribution of quantitative techniques including morphometry to renal diagnosis. *Ultrastruct Pathol* 2006;**30**:339–43. https://doi.org/10.1080/01913120600932537
5. Denic A, Bogojevic M, Mullan AF *et al.* Prognostic implications of a morphometric evaluation for chronic changes on all diagnostic native kidney biopsies. *JASN* 2022;**33**:1927–41. https://doi.org/10.1681/ASN.2022030234
6. Farris AB, Alpers CE. What is the best way to measure renal fibrosis?: a pathologist's perspective. *Kidney Int Suppl* 2014;**4**:9–15. https://doi.org/10.1038/kisup.2014.3
7. Farris AB, Adams CD, Brousaides N *et al.* Morphometric and visual evaluation of fibrosis in renal biopsies. *J Am Soc Nephrol* 2011;**22**:176–86. https://doi.org/10.1681/ASN.2009091005
8. Sethi S, D'Agati VD, Nast CC *et al.* A proposal for standardized grading of chronic changes in native kidney biopsy specimens. *Kidney Int* 2017;**91**:787–9. https://doi.org/10.1016/j.kint.2017.01.002
9. Asghar MS, Denic A, Mullan AF *et al.* Age-based versus young-adult thresholds for nephrosclerosis on kidney biopsy and prognostic implications for CKD. *JASN* 2023;**34**:1421–32. https://doi.org/10.1681/ASN.0000000000000171
10. Hughson MD, Johnson K, Young RJ *et al.* Glomerular size and glomerulosclerosis: relationships to disease categories, glomerular solidification, and ischemic obsolescence. *Am J Kidney Dis* 2002;**39**:679–88. https://doi.org/10.1053/ajkd.2002.31980
11. Kim T, Kwak Y, Lee JY *et al.* Pathological validation of the Japanese Renal Pathology Society classification and challenges in predicting renal prognosis in patients with diabetic nephropathy. *Kidney Res Clin Pract* 2022;**41**:545–55. https://doi.org/10.23876/j.krcp.22.123
12. Royal V, Leung N, Troyanov S *et al.* Clinicopathologic predictors of renal outcomes in light chain cast nephropathy: a multicenter retrospective study. *Blood* 2020;**135**:1833–46. https://doi.org/10.1182/blood.2019003807
13. Sasaki T, Tsuboi N, Okabayashi Y *et al.* Estimation of nephron number in living humans by combining

unenhanced computed tomography with biopsy-based stereology. *Sci Rep* 2019;**9**:14400. https://doi.org/10.1038/s41598-019-50529-x

14. Sasaki T, Tsuboi N, Kanzaki G *et al*. Biopsy-based estimation of total nephron number in Japanese living kidney donors. *Clin Exp Nephrol* 2019;**23**:629–37. https://doi.org/10.1007/s10157-018-01686-2

15. Denic A, Mathew J, Lerman LO *et al*. Single-nephron glomerular filtration rate in healthy adults. *N Engl J Med* 2017;**376**:2349–57. https://doi.org/10.1056/NEJMoa1614329

16. Denic A, Mullan AF, Alexander MP *et al*. An improved method for estimating nephron number and the association of resulting nephron number estimates with chronic kidney disease outcomes. *JASN* 2023;**34**:1264–78. https://doi.org/10.1681/ASN.0000000000000124

17. Fulladosa X, Moreso F, Narvaez JA *et al*. Estimation of total glomerular number in stable renal transplants. *J Am Soc Nephrol* 2003;**14**:2662–8. https://doi.org/10.1097/01.ASN.0000088025.33462.B0

18. Issa N, Vaughan LE, Denic A *et al*. Larger nephron size, low nephron number, and nephrosclerosis on biopsy as predictors of kidney function after donating a kidney. *Am J Transplant* 2019;**19**:1989–98. https://doi.org/10.1111/ajt.15259

19. Weibel ER, Gomez DM A principle for counting tissue structures on random sections. *J Appl Physiol* 1962;**17**:343–8. https://doi.org/10.1152/jappl.1962.17.2.343

20. Hughson M, Farris AB, 3rd, Douglas-Denton R *et al*. Glomerular number and size in autopsy kidneys: the relationship to birth weight. *Kidney Int* 2003;**63**:2113–22. https://doi.org/10.1046/j.1523-1755.2003.00018.x

21. Koike K, Ikezumi Y, Tsuboi N *et al*. Glomerular density and volume in renal biopsy specimens of children with proteinuria relative to preterm birth and gestational age. *CJASN* 2017;**12**:585–90. https://doi.org/10.2215/CJN.05650516

22. Tsuboi N, Kawamura T, Koike K *et al*. Glomerular density in renal biopsy specimens predicts the long-term prognosis of IgA nephropathy. *Clin J Am Soc Nephrol* 2010;**5**:39–44. https://doi.org/10.2215/CJN.04680709

23. Tsuboi N, Kawamura T, Ishii T *et al*. Changes in the glomerular density and size in serial renal biopsies during the progression of IgA nephropathy. *Nephrol Dial Transplant* 2009;**24**:892–9. https://doi.org/10.1093/ndt/gfn572

24. Denic A, Mathew J, Nagineni VV *et al*. Clinical and pathology findings associate consistently with larger glomerular volume. *JASN* 2018;**29**:1960–9. https://doi.org/10.1681/ASN.2017121305

25. Sasaki T, Tsuboi N, Okabayashi Y *et al*. Synergistic impact of diabetes and hypertension on the progression and distribution of glomerular histopathological lesions. *Am J Hypertens* 2019;**32**:900–8. https://doi.org/10.1093/ajh/hpz059

26. Haruhara K, Tsuboi N, Kanzaki G *et al*. Glomerular density in biopsy-proven hypertensive nephrosclerosis. *AJHYPE* 2015;**28**:1164–71. https://doi.org/10.1093/ajh/hpu267

27. Tsuboi N, Utsunomiya Y, Koike K *et al*. Factors related to the glomerular size in renal biopsies of chronic kidney disease patients. *CN* 2013;**79**:277–84. https://doi.org/10.5414/CN107817

28. Tsuboi N, Utsunomiya Y, Kanzaki G *et al*. Low glomerular density with glomerulomegaly in obesity-related glomerulopathy. *Clin J Am Soc Nephrol* 2012;**7**:735–41. https://doi.org/10.2215/CJN.07270711

29. Okamoto H, Kawamura T, Okonogi H *et al*. The role of a low glomerular density and being overweight in the etiology of proteinuria in CKD patients without known glomerular diseases. *Clin Exp Nephrol* 2014;**18**:911–7. https://doi.org/10.1007/s10157-014-0940-y

30. Okabayashi Y, Tsuboi N, Sasaki T *et al*. Single-nephron GFR in patients with obesity-related glomerulopathy. *Kidney Int Rep* 2020;**5**:1218–27. https://doi.org/10.1016/j.ekir.2020.05.013

31. Denic A, Ricaurte L, Lopez CL *et al*. Glomerular volume and glomerulosclerosis at different depths within the human kidney. *JASN* 2019;**30**:1471–80. https://doi.org/10.1681/ASN.2019020183

32. Haruhara K, Kanzaki G, Sasaki T *et al*. Associations between nephron number and podometrics in human kidneys. *Kidney Int* 2022;**102**:1127–35. https://doi.org/10.1016/j.kint.2022.07.028

33. Issa N, Lopez CL, Denic A *et al*. Kidney structural features from living donors predict graft failure in the recipient. *JASN* 2020;**31**:415–23. https://doi.org/10.1681/ASN.2019090964

34. Merzkani MA, Denic A, Narasimhan R *et al*. Kidney microstructural features at the time of donation predict long-term risk of chronic kidney disease in living kidney donors. *Mayo Clin Proc* 2021;**96**:40–51. https://doi.org/10.1016/j.mayocp.2020.08.041

35. Lopes JA, Moreso F, Riera L *et al*. Evaluation of preimplantation kidney biopsies: comparison of Banff criteria to a morphometric approach. *Kidney Int* 2005;**67**:1595–600. https://doi.org/10.1111/j.1523-1755.2005.00241.x

36. Sasaki T, Tsuboi N, Haruhara K *et al*. Bowman capsule volume and related factors in adults with normal renal function. *Kidney Int Rep* 2018;**3**:314–20. https://doi.org/10.1016/j.ekir.2017.10.007

37. Haruhara K, Tsuboi N, Sasaki T *et al*. Volume ratio of glomerular tufts to Bowman capsules and renal outcomes in nephrosclerosis. *Am J Hypertens* 2019;**32**:45–53. https://doi.org/10.1093/ajh/hpy147

38. Haruhara K, Sasaki T, de Zoysa N *et al*. Podometrics in Japanese living donor kidneys: associations with nephron number, age, and hypertension. *JASN* 2021;**32**:1187–99. https://doi.org/10.1681/ASN.2020101486

39. Okabayashi Y, Tsuboi N, Kanzaki G *et al*. Aging vs. hypertension: an autopsy study of sclerotic renal histopathological lesions in adults with normal renal function. *Am J Hypertens* 2019;**32**:676–83. https://doi.org/10.1093/ajh/hpz040

40. Niznik RS, Lopez CL, Kremers WK *et al*. Global glomerulosclerosis in kidney biopsies with differing amounts of cortex: a clinical-Ppathologic correlation study. *Kidney Medicine* 2019;**1**:153–61. https://doi.org/10.1016/j.xkme.2019.05.004

41. Kremers WK, Denic A, Lieske JC *et al*. Distinguishing age-related from disease-related glomerulosclerosis on kidney biopsy: the Aging Kidney Anatomy study. *Nephrol Dial Transplant* 2015;**30**:2034–9. https://doi.org/10.1093/ndt/gfv072

42. Koike K, Tsuboi N, Utsunomiya Y *et al*. Glomerular density-associated changes in clinicopathological features of minimal change nephrotic syndrome in adults. *Am J Nephrol* 2011;**34**:542–8. https://doi.org/10.1159/000334360

43. Tsuboi N, Kawamura T, Miyazaki Y *et al*. Low glomerular density is a risk factor for progression in idiopathic membranous nephropathy. *Nephrol Dial Transplant* 2011;**26**:3555–60. https://doi.org/10.1093/ndt/gfr399

44. Amano H, Koike K, Haruhara K *et al*. Time-averaged proteinuria during follow-up and renal prognosis in patients with biopsy-proven benign nephrosclerosis. *Clin Exp Nephrol* 2020;**24**:688–95. https://doi.org/10.1007/s10157-020-01885-w

45. Hommos MS, Zeng C, Liu Z *et al.* Global glomerulosclerosis with nephrotic syndrome; the clinical importance of age adjustment. *Kidney Int* 2018;**93**:1175–82. https://doi.org/10.1016/j.kint.2017.09.028

46. Denic A, Bogojevic M, Subramani R *et al.* Changes in glomerular volume, sclerosis, and ischemia at 5 years after kidney transplantation: incidence and correlation with late graft failure. *JASN* 2023;**34**:346–58. https://doi.org/10.1681/ASN.2022040418

47. Street JM, Souza AC, Alvarez-Prats A *et al.* Automated quantification of renal fibrosis with Sirius Red and polarization contrast microscopy. *Physiol Rep* 2014;**2**:e12088. https://doi.org/10.14814/phy2.12088

48. Keijbeck A, Raaijmaakers A, Hillen L *et al.* Visual interstitial fibrosis assessment as continuous variable in protocol renal transplant biopsies. *Histopathology* 2023;**82**:713–21. https://doi.org/10.1111/his.14857

49. Farris AB, Ellis CL, Rogers TE *et al.* Renal medullary and cortical correlates in fibrosis, epithelial mass, microvascularity, and microanatomy using whole slide image analysis morphometry. *PLoS One* 2016;**11**:e0161019. https://doi.org/10.1371/journal.pone.0161019

50. Ricaurte Archila L, Denic A, Mullan AF *et al.* A higher foci density of interstitial fibrosis and tubular atrophy predicts progressive CKD after a radical nephrectomy for tumor. *JASN* 2021;**32**:2623–33. https://doi.org/10.1681/ASN.2021020267

51. Helgeson ES, Mannon R, Grande J *et al.* i-IFTA and chronic active T cell-mediated rejection: a tale of 2 (DeKAF) cohorts. *Am J Transplant* 2021;**21**:1866–77. https://doi.org/10.1111/ajt.16352

52. Gaston RS. Chronic calcineurin inhibitor nephrotoxicity: reflections on an evolving paradigm. *Clin J Am Soc Nephrol* 2009;**4**:2029–34. https://doi.org/10.2215/CJN.03820609

53. Denic A, Lieske JC, Chakkera HA *et al.* The substantial loss of nephrons in healthy human kidneys with aging. *JASN* 2017;**28**:313–20. https://doi.org/10.1681/ASN.2016020154

54. Denic A, Morales MC, Park WD *et al.* Using computer-assisted morphometrics of 5-year biopsies to identify biomarkers of late renal allograft loss. *Am J Transplant* 2019;**19**:2846–54. https://doi.org/10.1111/ajt.15380

55. Roufosse C, Simmonds N, Clahsen-van Groningen M *et al.* A 2018 reference guide to the Banff classification of renal allograft pathology. *Transplantation* 2018;**102**:1795–814. https://doi.org/10.1097/TP.0000000000002366

56. Marini MB, Rocha LP, Machado JR *et al.* Contribution of glomerular morphometry to the diagnosis of pediatric nephropathies. *Saudi J Kidney Dis Transpl* 2016;**27**:493–9. https://doi.org/10.4103/1319-2442.182382

57. Sharma A, Gupta R, Bagga A *et al.* Glomerular filtration barrier in pediatric idiopathic nephrotic syndrome. *Saudi J Kidney Dis Transpl* 2013;**24**:286–91. https://doi.org/10.4103/1319-2442.109577

58. Gupta R, Sharma A, Gupta R *et al.* Morphometry of non-inflammatory arteriolar changes in lupus nephritis: a study of 40 cases. *Saudi J Kidney Dis Transpl* 2012;**23**:1196–201. https://doi.org/10.4103/1319-2442.103559

59. Das P, Sharma A, Gupta R *et al.* Histomorphological classification of focal segmental glomerulosclerosis: a critical evaluation of clinical, histologic and morphometric features. *Saudi J Kidney Dis Transpl* 2012;**23**:1008–16. https://doi.org/10.4103/1319-2442.100883

60. Derewicz D, Moldovan VT, Ali L *et al.* The role of glomerular morphometric features in pediatric podocytopathies—a single center study. *Rom J Morphol Embryol* 2018;**59**:1061–6.

61. Kashif AW, Verma N, Verma S *et al.* Utility of glomerular morphometry in diagnosing pediatric renal disease. *Medical Journal Armed Forces India* 2021;**77**:194–9. https://doi.org/10.1016/j.mjafi.2020.08.007

62. Athanazio DA, Sweet GM, Silva CA *et al.* Semiquantitative and semi-automated morphometric evaluation of chronic lesions in renal biopsies. *Int Urol Nephrol* 2009;**41**:643–51. https://doi.org/10.1007/s11255-008-9494-9

63. Danilewicz M, Wagrowska-Danielwicz M. Morphometric and immunohistochemical insight into focal segmental glomerulosclerosis in obese and non-obese patients. *Nefrologia* 2009;**29**:35–41. https://doi.org/10.3265/Nefrologia.2009.29.1.35.1.en.full.pdf

64. Smoyer WE, Gregory MJ, Bajwa RS *et al.* Quantitative morphometry of renal biopsies prior to cyclosporine in nephrotic syndrome. *Pediatr Nephrol* 1998;**12**:737–43. https://doi.org/10.1007/s004670050536

65. Sasaki T, Tsuboi N, Marumoto H *et al.* Nephron number and time to remission in steroid-sensitive minimal change disease. *Kidney Medicine* 2020;**2**:559–568.e1 e551. https://doi.org/10.1016/j.xkme.2020.05.011

66. Gupte PA, Vaideeswar P, Kandalkar BM. Cyanotic nephropathy—a morphometric analysis. *Congenit Heart Dis* 2014;**9**:280–5. https://doi.org/10.1111/chd.12121

67. Rayat CS, Joshi K, Dey P *et al.* Glomerular morphometry in biopsy evaluation of minimal change disease, membranous glomerulonephritis, thin basement membrane disease and Alport's syndrome. *Anal Quant Cytol Histol* 2007;**29**:173–82.

68. Kanzaki G, Puelles VG, Cullen-McEwen LA *et al.* New insights on glomerular hyperfiltration: a Japanese autopsy study. *JCI Insight* 2017;**2**:1–11. https://doi.org/10.1172/jci.insight.94334

69. Kobayashi A, Yamamoto I, Katsumata H *et al.* Change in glomerular volume and its clinicopathological impact after kidney transplantation. *Nephrology* 2015;**20**:31–35. https://doi.org/10.1111/nep.12463

70. Hamada AM, Yamamoto I, Nakada Y *et al.* Association between GLCCI1 promoter polymorphism (Rs37972) and post-transplant hypertension in renal transplant recipients. *Kidney Blood Press Res* 2017;**42**:1155–63. https://doi.org/10.1159/000485862

71. Yamakawa T, Kobayashi A, Yamamoto I *et al.* Clinical and pathological features of donor/recipient body weight mismatch after kidney transplantation. *Nephrology* 2015;**20**:36–39. https://doi.org/10.1111/nep.12470

72. Marumoto H, Tsuboi N, D'Agati VD *et al.* Total nephron number and single-nephron parameters in patients with IgA nephropathy. *Kidney360* 2021;**2**:828–41. https://doi.org/10.34067/KID.0006972020

73. Oba R, Kanzaki G, Sasaki T *et al.* Dietary protein intake and single-nephron glomerular filtration rate. *Nutrients* 2020;**12**:2549. https://doi.org/10.3390/nu12092549

74. Okabayashi Y, Tsuboi N, Sasaki T *et al.* Glomerulopathy associated with moderate obesity. *Kidney International Reports* 2016;**1**:250–5. https://doi.org/10.1016/j.ekir.2016.08.006

75. Wavamunno MD, O'Connell PJ, Vitalone M *et al.* Transplant glomerulopathy: ultrastructural abnormalities occur early in longitudinal analysis of protocol biopsies. *Am J Transplant* 2007;**7**:2757–68. https://doi.org/10.1111/j.1600-6143.2007.01995.x

76. Howie AJ, Ferreira MA, Adu D. Prognostic value of simple measurement of chronic damage in renal biopsy specimens. *Nephrol Dial Transplant* 2001;**16**:1163–9. https://doi.org/10.1093/ndt/16.6.1163

77. Hunter MG, Hurwitz S, Bellamy CO *et al*. Quantitative morphometry of lupus nephritis: the significance of collagen, tubular space, and inflammatory infiltrate. *Kidney Int* 2005;**67**:94–102. https://doi.org/10.1111/j.1523-1755.2005.00059.x

78. Viola PCL, Felaco P, Lattanzio G *et al*. Prognostic value of morphologic and morphometric analyses in IgA nephropathy biopsies. *Transl Med Commun* 2016;**1**:1–10. https://doi.org/10.1186/s41231-016-0007-z.

79. Lemley KV, Bagnasco SM, Nast CC *et al*. Morphometry predicts early GFR change in primary proteinuric glomerulopathies: a longitudinal cohort study using generalized estimating equations. *PLoS One* 2016;**11**:e0157148. https://doi.org/10.1371/journal.pone.0157148

80. Paraskevakou H, Kavantzas N, Pavlopoulos PM *et al*. Membranous glomerulonephritis: a morphometric study. *Pathol Res Pract* 2000;**196**:141–4. https://doi.org/10.1016/S0344-0338(00)80093-X

81. Horvatic I, Ljubanovic DG, Bulimbasic S *et al*. Prognostic significance of glomerular and tubulointerstitial morphometry in idiopathic membranous nephropathy. *Pathol Res Pract* 2012;**208**:662–7. https://doi.org/10.1016/j.prp.2012.08.004

82. Fufaa GD, Weil EJ, Lemley KV *et al*. Structural predictors of loss of renal function in American Indians with type 2 diabetes. *Clin J Am Soc Nephrol* 2016;**11**:254–61. https://doi.org/10.2215/CJN.05760515

83. Dao M, Pouliquen C, Duquesne A *et al*. Usefulness of morphometric image analysis with Sirius Red to assess interstitial fibrosis after renal transplantation from uncontrolled circulatory death donors. *Sci Rep* 2020;**10**:6894. https://doi.org/10.1038/s41598-020-63749-3

84. Wang W, Yu Y, Wen J *et al*. Combination of functional magnetic resonance imaging and histopathologic analysis to evaluate interstitial fibrosis in kidney allografts. *CJASN* 2019;**14**:1372–80. https://doi.org/10.2215/CJN.00020119.

85. Zhang J, Yu Y, Liu X *et al*. Evaluation of renal fibrosis by mapping histology and magnetic resonance imaging. *Kidney Dis* 2021;**7**:131–42. https://doi.org/10.1159/000513332

86. Mafune Hamada A, Yamamoto I, Kawabe M *et al*. Interstitial fibroblasts in donor kidneys predict late posttransplant anemia. *Clin Kidney J* 2021;**14**:132–8. https://doi.org/10.1093/ckj/sfz122

87. Tewari RSV, Boruah D, Mendonca S *et al*. Evaluation of fibrosis in renal biopsies by morphometric analysis and visual analysis and its correlation with renal function. *Immunopathol Persa* 2017;**3**:e06. https://immunopathol.com/PDF/ipp-3-e06.pdf

88. Asghar MS, Denic A, Mullan AF *et al*. Age-based versus young-adult thresholds for nephrosclerosis on kidney biopsy and prognostic implications for chronic kidney disease. *JASN* 2023;**34**:1421–32. https://doi.org/10.1681/ASN.0000000000000171